



OPEN

Bexarotene-induced cell death in ovarian cancer cells through Caspase-4-gasdermin E mediated pyroptosis

Tatsuya Kobayashi¹, Akira Mitsuhashi^{1,2✉}, Piao Hongying¹, Masashi Shioya^{1,3}, Katsushi Kojima³, Kyoko Nishikimi¹, Kinnosuke Yahiro⁴ & Makio Shozu¹

Bexarotene selectively activates retinoid X receptor, which is a commonly used anticancer agent for cutaneous T-cell lymphoma. In this study, we aimed to investigate the anticancer effect of bexarotene and its underlying mechanism in ovarian cancer in vitro. The ES2 and NIH:OVACAR3 ovarian cancer cell lines were treated with 0, 5, 10, or 20 μM of bexarotene. After 24 h, cell number measurement and lactate dehydrogenase (LDH) cytotoxicity assay were performed. The effect of bexarotene on CDKN1A expression, cell cycle-related protein, cell cycle, pyroptosis, and apoptosis was evaluated. Bexarotene reduced cell proliferation in all concentrations in both the cells. At concentrations of $>10 \mu\text{M}$, extracellular LDH activity increased with cell rupture. Treatment using $10 \mu\text{M}$ of bexarotene increased CDKN1A mRNA levels, decreased cell cycle-related protein expression, and increased the sub-G1 cell population in both cells. In ES2 cells, caspase-4 and GSDME were activated, whereas caspase-3 was not, indicating that bexarotene-induced cell death might be pyroptosis. A clinical setting concentration of bexarotene induced cell death through caspase-4-mediated pyroptosis in ovarian cancer cell lines. Thus, bexarotene may serve as a novel therapeutic agent for ovarian cancer.

Ovarian cancer is the fifth most common cause of cancer-related death and the most deadly gynecological cancer in western countries¹. Although the initial clinical response is generally satisfactory, more than 70% of affected patients experience recurrences and ultimately die. Multimodality treatment with cytoreductive surgery and platinum-taxane-based chemotherapy combined with molecularly targeted drugs has shown prolonged survival. However, the overall cure rate of the disease has not considerably changed. Therefore, additional treatment strategies that can improve survival are urgently required.

Retinoid X receptor (RXR) is a member of nuclear receptor family. RXR acts as a transcriptional factor by homodimerizing with itself or other nuclear receptor families when stimulated by their specific ligands. Bexarotene (LGD1069, Targretin[®]) is an RXR-selective agonist that binds and activates all three RXR isoforms (RXR α , RXR β , and RXR γ) with equivalent affinity and potency². Bexarotene is approved by the FDA and is a widely used drug for treating cutaneous manifestations in cutaneous T-cell lymphoma (CTCL)³. Moreover, this drug has gained increasing attention in cancer treatment; hence, it has been used as an off-label drug for non-small cell lung cancer⁴ and breast cancer⁵. In vitro studies have shown that bexarotene can also prevent and overcome acquired drug resistance in advanced breast cancer^{6,7}, non-small cell lung cancer^{8,9}, and even advanced prostate cancer¹⁰. An in vitro analysis revealed that bexarotene could kill cancer cells via apoptosis, decrease TGF- α and EGFR expressions, induce cellular senescence associated with increased p21 and p16 expressions, and promote G1 phase cell cycle arrest¹¹. However, the precise mechanism of cell proliferation inhibition by bexarotene remains unclear.

Pyroptosis is one of the regulated cell deaths triggered by certain caspases that are mainly activated by inflammation, anticancer drugs, and endoplasmic reticulum (ER) stress. Inflammatory caspases (caspase-1/4/5 in humans) cleave gasdermin D (GSDMD), which is required and sufficient for pyroptosis^{12,13}. The polymerized GSDMD N-terminal forms pores in the cell membrane to increase permeability and osmosis, thereby causing

¹Department of Reproductive Medicine, Graduate School of Medicine, Chiba University, Inohana 1-8-1, Chuo-ku, Chiba 260-8670, Japan. ²Department of Obstetrics and Gynecology, School of Medicine, Dokkyo Medical University, Tochigi 321-0293, Japan. ³Takahashi Women's Clinic, Chiba 260-0028, Japan. ⁴Department of Microbiology and Infection Control Sciences, Division of Biological Sciences, Kyoto Pharmaceutical University, Kyoto 607-8412, Japan. ✉email: a-mitsu@dokkyomed.ac.jp

cell rupture, which is a characteristic of pyroptosis. Caspase-3, a well-known apoptotic caspase, causes pyroptosis with gasdermin E (GSDME/DFNA5). Chemotherapy drugs such as cisplatin, etoposide, and doxorubicin induce pyroptosis in tumor cells with high GSDME levels caused by caspase-3¹⁴. Several anticancer drugs, such as chemotherapy drugs and miRNA, can reduce tumor viability and invasiveness by inducing tumor pyroptosis¹⁵. Hence, pyroptosis induction might be a potent anticancer drug target¹⁶.

In epithelial ovarian cancer, retinoic acid receptors are frequently and strongly expressed and may indicate an adverse prognosis¹⁷. Therefore, RXR-selective retinoids, such as bexarotene, might potentially treat ovarian cancer; however, the effect of bexarotene on ovarian cancer remains unclear. Hence, this study aimed to investigate whether bexarotene could suppress the proliferation of ovarian cancer cells in vitro and better understand the antitumorigenic potential of bexarotene by exploring the precise mechanism of bexarotene on cell death, particularly pyroptosis.

Methods

Cell culture. The ovarian clear cell carcinoma cell line (ES2) and serous ovarian carcinoma cell line (NIH:OVACAR3) were used. ES2 and NIH:OVACAR-3 cell lines were purchased from ATCC (Manassas, VA, USA) and RIKEN BioResource Center (Tsukuba, Japan). These ovarian cancer cell lines were routinely cultured in RPMI 1640 (Nacalai Tesque, Kyoto, Japan) containing inactivated 2% fetal bovine serum (Equitech-Bio, Kerrville, TX, USA) and 1% penicillin–streptomycin (Nacalai Tesque) at 37 °C with 5% CO₂ in room air.

Cell proliferation assay and lactate dehydrogenase (LDH) cytotoxicity assay. In the culture medium, we seeded the cells in 12-well plates (100,000 cells/well). At 80% confluence, the cells were treated with 0–20 μM of bexarotene (Tokyo Chemical Industry Co., Ltd., Tokyo, Japan) dissolved in dimethyl sulfoxide (Fujifilm Wako, Osaka, Japan) for 24 h. Bexarotene is insoluble in water; hence, it was dissolved in dimethyl sulfoxide (DMSO). Therefore, all the experiments, including the untreated control, were performed with a concentration of 0.1% DMSO. The cells were then treated with trypsin–EDTA solution (Nacalai Tesque) and mixed with the total amount of trypan blue solution (Nacalai Tesque). Subsequently, the live cells were counted using a cell-counting chamber (WakenBtech Co., Ltd., Kyoto, Japan) under a stereomicroscope (Olympus, Tokyo, Japan).

Moreover, we collected the cell culture supernatant and measured the LDH activity using the LDH Cytotoxicity Assay Kit (Nacalai Tesque) according to the manufacturer's protocol. The LDH levels of the cell culture supernatant derived from the bexarotene-treated cell group were normalized relative to the cultured medium derived from the control group (vehicle of the bexarotene-treated group). Each experiment was repeated at least three times, and the LDH activity was compared to that of the control group.

Protein extraction and western blot. We washed the cultured cells with PBS and extracted the total protein using a complete Lysis-M reagent (Roche, Basel, Switzerland) containing 1% Halt™ Phosphatase Inhibitor Cocktail (Thermo Fisher Science, Waltham, MA, USA) for 15 min at room temperature. We subsequently centrifuged the cell lysate at 15,000×g for 15 min at 4 °C, separated 7.5 μg of total protein in 10% or 4–15% gradient SDS-PAGE (Bio-Rad, Hercules, CA, USA), and transferred it to a polyvinylidene fluoride (PVDF) membrane (Merck Millipore, Burlington, MA, USA). Nonspecific binding to the PVDF membrane was blocked in Blocking one-P solution (Nacalai Tesque) at room temperature for 30 min. The first antibody was reacted at 4 °C for overnight. Subsequently, we washed the PVDF membrane in PBS-T and enhanced the protein signal by anti-mouse or rabbit IgG antibody (1/10,000 or 5000) at room temperature for 1 h. We used ECL select (Roche) or ECL Prime reagent (Roche) to detect protein signals. A densitometric analysis of western blot was performed using a densitometer (CS analyzer version 3.0 software, ATTO, Tokyo, Japan), and the intensity was normalized to the b-actin protein levels.

RNA extraction and real-time quantitative PCR. Total RNA from cultured cells was extracted using the RNeasy Mini Kits (Qiagen, Hilden, Germany) according to the manufacturer's protocol. Using the SuperScript VILO cDNA Synthesis Kit (Thermo Fisher Science, Waltham, MA, USA), we reverse-transcribed the extracted RNA into complementary DNA (cDNA). Real-time quantitative PCR (RT-qPCR) was conducted using Light Cycler DNA Master SYBR Green I Kit (F. Hoffmann–Roche Ltd., Basel, Switzerland) with Light Cycler Nano System (F. Hoffmann–Roche Ltd). Furthermore, we evaluated the *CDKN1A* and *GAPDH* (internal control) mRNA expression levels. The expression levels of measured genes were normalized relative to that of *GAPDH* mRNA. The $2^{-\Delta\Delta C_q}$ method was used to obtain the relative quantitative value¹⁸. Supplementary Table S1 lists the gene-specific primers.

Cell cycle analysis. Vehicle or 10 μM–bexarotene-treated cells were cultured for 48 h and then harvested by trypsin–EDTA solution. The cells were washed twice with PBS and fixed with 70% ethanol (Fujifilm Wako) at –30 °C until cell cycle analysis. Following this, cells were incubated in 20 μg/ml RNase for 30 min after staining with 50 μg/ml propidium iodide (PI) solution (Nacalai tesque) at 4 °C for 30 min in darkness. Fluorescence intensity was analyzed using CytoFLEX flow cytometer (BECKMAN COULTER, Brea, CA, USA) with CytEX-pert Soft wear (BECKMAN COULTER). We analyzed 15,000 events to determine the cell cycle phase and classified cells into sub-G1, G0/G1, S, or G2/M phases according to the fluorescence intensity of the cells.

Small interfering RNA (siRNA) transfection. Using Lipofectamine RNAiMAX (Thermo Fisher Science, Waltham, MA, USA), we transfected ES2 cell lines with a siRNA. The si-protein kinase R-like ER kinase (PERK; SI02223718; Qiagen, Hilden, Germany) RNA, si-inositol-requiring enzyme 1-A (IRE1A; SI00605255;

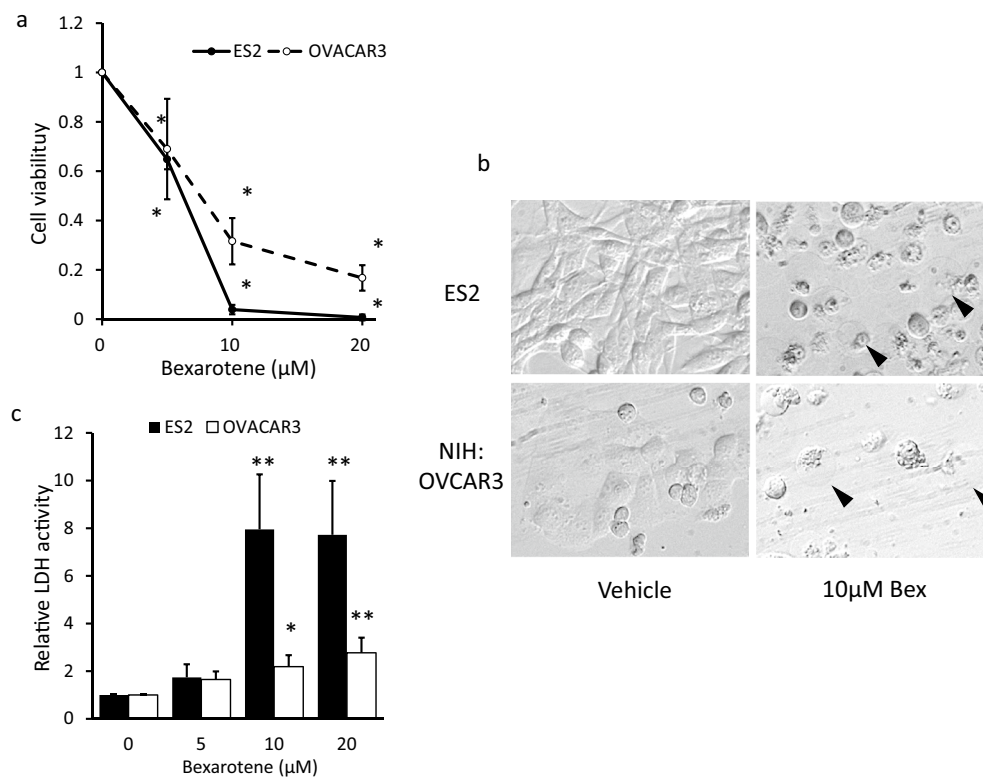


Figure 1. Bexarotene treatment reduced cell viability and induced cell death by LDH release and plasma membrane bursting. **(a)** In ES2 and NIH:OVACAR3 cells, counted manually were cell numbers after 24 h of bexarotene treatment. Measured was the cell viability against the bexarotene nontreated group. The results presented were the mean, \pm standard deviation for at least three independent experiments. **(b)** Morphological analysis of ES2 cells (upper two panels) and NIH:OVACAR3 (lower two panels). The plasma membrane expanded, and the broken cells had a swollen structure (arrow). **(c)** Bexarotene treatment was extracellular LDH activity. The results presented were the mean \pm standard deviation for at least three independent experiments. * $p < 0.05$, ** $p < 0.01$, compared with bexarotene-free control. LDH, lactate dehydrogenase.

Qiagen), or a non-target siRNA (control) were used. To prepare the siRNA transfection solution for each tube, we mixed 5 pmol of siRNA with 50 μ L of Opti-MEM reduced-serum medium (Thermo Fisher Science, Waltham, MA, USA). Concurrently, we mixed 1 μ L of Lipofectamine RNAiMAX with 50 μ L of Opti-MEM. Following this, the two solutions were mixed by gentle pipetting and incubated for 5 min at room temperature to allow siRNA/lipid complexes to form. The treated cells forming siRNA/lipid complexes were then incubated for 48 h at 37 $^{\circ}$ C, followed by bexarotene treatment.

Antibodies and other reagents. For detecting the target protein, we used an anti-caspase-4 antibody (1/1000; MBL, Tokyo, Japan), anti-caspase-3 (D175) antibody (1/1000; Cell Signaling Technology, Danvers, MA, USA), anti-GSDME antibody (1/1000; Proteintech Group, Rosemont, IL, USA), anti-cyclin D1 antibody (1/1000; Cell Signaling Technology), anti-Rb antibody (1/1000; Cell Signaling Technology), anti-phospho-Rb antibody, anti-CDK4 antibody (1/1000; Cell Signaling Technology), anti-CDK6 antibody (1/1000; Cell Signaling Technology), anti-PERK antibody (1/1000; Cell Signaling Technology), and anti- β actin antibody (1/5000; Cell Signaling Technology) as the first antibodies.

We used ZYVAD-FMK (R&D SYSTEMS, Minneapolis, MN, USA) dissolved in dimethyl sulfoxide (Sigma-Aldrich, St. Louis, MO, USA) for caspase-4 inhibition experiments.

Statistical analysis. The cell proliferation assay was statistically analyzed using an independent *t*-test. All comparisons were performed using a two-sided test. In addition, $P < 0.05$ was considered statistically significant. All statistical data were analyzed using the JMP statistical software (SAS Institute Inc., Cary, NC, USA).

Results

Bexarotene reduced cell viability and affected cell shape. First, we examined the effect of bexarotene treatment on cell viability, cell membrane damage, and cell morphological shape to determine whether bexarotene had anticancer potential against ovarian cancer cell lines. After 24 h of bexarotene treatment, cell viability was significantly reduced dose-dependently in both the ES2 and NIH:OVACAR3 cells (Fig. 1a), and the morphology in cancer cells drastically changed, as observed microscopically (Fig. 1b). Furthermore, bexarotene-

treated cells were detached from the surface of the culture dish, and the plasma membrane clearly expanded. Moreover, some cells exhibited a post-cell burst appearance ($\geq 10 \mu\text{M}$ of bexarotene).

The effect of bexarotene on plasma membrane damage was evaluated by measuring the released LDH activity in the culture supernatant. In living cells, LDH is present in the cytoplasm, but it is released extracellularly due to cell membrane changes that occur during the cell death processes, such as in necroptosis and pyroptosis¹⁹. The levels of released LDH significantly increased in the 10 and 20 μM -bexarotene-treated group compared with the control group in ES2 cells (Fig. 1c, $P < 0.05$). Likewise, the LDH levels in NIH:OVACAR3 cells also significantly increased in the 10 and 20 μM -bexarotene-treated group ($P < 0.05$). These results indicated that bexarotene induced cell death by causing plasma membrane damage in ovarian cancer cell lines.

Bexarotene increased p21 mRNA expression and induced cell growth inhibition with sub-G1 arrest. Tanaka et al. reported that a ligand-activated RXR homodimer upregulates cyclin-dependent kinase inhibitor p21 (CDKN1A) expression by directly binding to its promoter region and regulating cell proliferation²⁰. Therefore, we evaluated whether bexarotene reduced the cell viability by acting as an RXR agonist in ovarian cancer cell lines.

First, we measured the mRNA expression levels of *RXR- α* , *RXR- β* , and *RXR- γ* in ES2 and NIH:OVACAR-3 cells using RT-PCR to confirm the RXR expression. The *RXR- α* and *RXR- β* mRNA were expressed, but *RXR- γ* mRNA was not in both cells (data not shown). Then, to determine whether bexarotene acted as an RXR agonist in ovarian cancer cell lines, we measured the *CDKN1A* mRNA expression levels after 24 h of bexarotene treatment. In both the cell lines, the administration of 10 μM bexarotene increased *CDKN1A* mRNA expression by approximately twofold (Fig. 2a, b).

Subsequently, the levels of cell cycle-related proteins, specifically the downstream of p21 protein, CDK4, CDK6, Cyclin D1, and phospho-RB, were examined using western blot in 10 μM -bexarotene-treated cells²¹. After 48 h of bexarotene treatment, the levels of CDK4, CDK6, Cyclin D1, and phospho-RB decreased in both ovarian cancer cell lines (Fig. 2c, d, S2).

Finally, we performed cell cycle analysis with both the PI-stained cell lines after 48 h from bexarotene treatment using flow cytometry analysis. Bexarotene treatment significantly increased the population of the sub-G1 phase and reduced the population of G0/G1 and G2/M phase cells in both the cell lines (Fig. 2e, f).

Bexarotene-induced pyroptosis via caspase-4 and GSDME-related pathway. As above, bexarotene-treated ovarian cancer cell lines exhibited drastic morphological changes with the release of intracellular LDH. The swelling structure formation and membrane rupture during cell death are related to pyroptosis^{12,22}. Thus, the bexarotene-induced cell death might be pyroptosis. We used ES2 cells, which were highly sensitive to bexarotene, to determine whether bexarotene induces pyroptosis in ovarian cancer cells. To determine whether the expression and activation of caspase-1 and -4 are caused by bexarotene stimulation at molecular levels, we performed western blot using an antibody specific to caspase-1 and -4. In ES2 cells, caspase-4 was expressed and activated after 24 h of 10- μM -bexarotene treatment (Fig. 3a, b). Meanwhile, caspase-1 mRNA and protein were not detected in the ES2 cell line (data not shown). Furthermore, Bexarotene stimulation could not activate caspase-3, the apoptosis-related caspase (Fig. S3A). During pyroptosis, the activated caspase cleaves GSDM and the N-terminal domain dimer of GSDM induces cell membrane perforation²³. Therefore, we also evaluated GSDME and GSDMD cleavage using western blot. From 24 h after the start of bexarotene treatment, we detected the cleaved GSDME (Fig. 3a, c). Meanwhile, bexarotene treatment did not cleave GSDMD (Fig. 3a).

We then evaluated whether 10 μM -ZYVAD-FMK (caspase-4 inhibitor) pretreatment can affect pyroptosis. ZYVAD-FMK reduces the cleaved GSDME levels at 4 h after the bexarotene treatment (Fig. 3d, S2B). These results indicated that cleaved GSDME was related to caspase-4 activation. Subsequently, we evaluated whether 10 μM -ZYVAD-FMK pretreatment can mitigate bexarotene-induced cell viability reduction and LDH release into the culture media after 24 h of bexarotene treatment. The pretreatment of ZYVAD-FMK partially attenuated the bexarotene-induced morphological changes in ES2 cells (Fig. 3e). However, as shown in Fig. 3f, pretreatment with ZYVAD-FMK could not restore bexarotene-induced cell viability reduction ($P = 0.7742$, bexarotene-treated group vs. bexarotene with ZYVAD-FMK-treated group). Meanwhile, pretreatment with ZYVAD-FMK suppressed the increase in extracellular LDH levels induced by bexarotene (Fig. 3g; bexarotene-treated group vs. bexarotene with ZYVAD-FMK-treated group; $P < 0.05$). These results indicate that bexarotene has two functions on ovarian cancer cells: cell proliferation suppression and caspase-4 GSDME-related pyroptosis, and these are independent actions.

Bexarotene-induced ER stress, which is not associated with pyroptosis. The ER stress might cause pyroptotic cell death in several cells in vitro^{24,25}. Thus, we examined whether bexarotene-induced ER stress in ES2 cells. We also evaluated whether bexarotene activated the unfolded protein response (UPR) signaling pathways, which are common ER stress markers, in ES2 cells. In this study, we used PERK phosphorylation, and X-binding protein 1 (XBP1) mRNA splicing as ER stress response markers.

Spliced XBP1 worked as a transcriptional factor for upregulating or downregulating the UPR-related gene under ER stress conditions. From 2 h after bexarotene treatment, *XBP1* mRNA was spliced in an increased time-dependent manner (Fig. 4a, S4A). After 2 h of bexarotene treatment, the molecular weight of PERK was rapidly shifted to a higher molecular form (Fig. 4b, c, S4B), indicating that PERK protein was activated via phosphorylation. These results indicated that bexarotene rapidly induced ER stress in ES2 cells. Subsequently, we examined whether the knockdown of ER stress sensor proteins attenuated the cell death caused by bexarotene in ES2 cells. We found that PERK and IRE1 knockdown could not attenuate the release of LDH (Fig. 4d) and restore cell morphological changes (Fig. 4e) caused by bexarotene treatment.

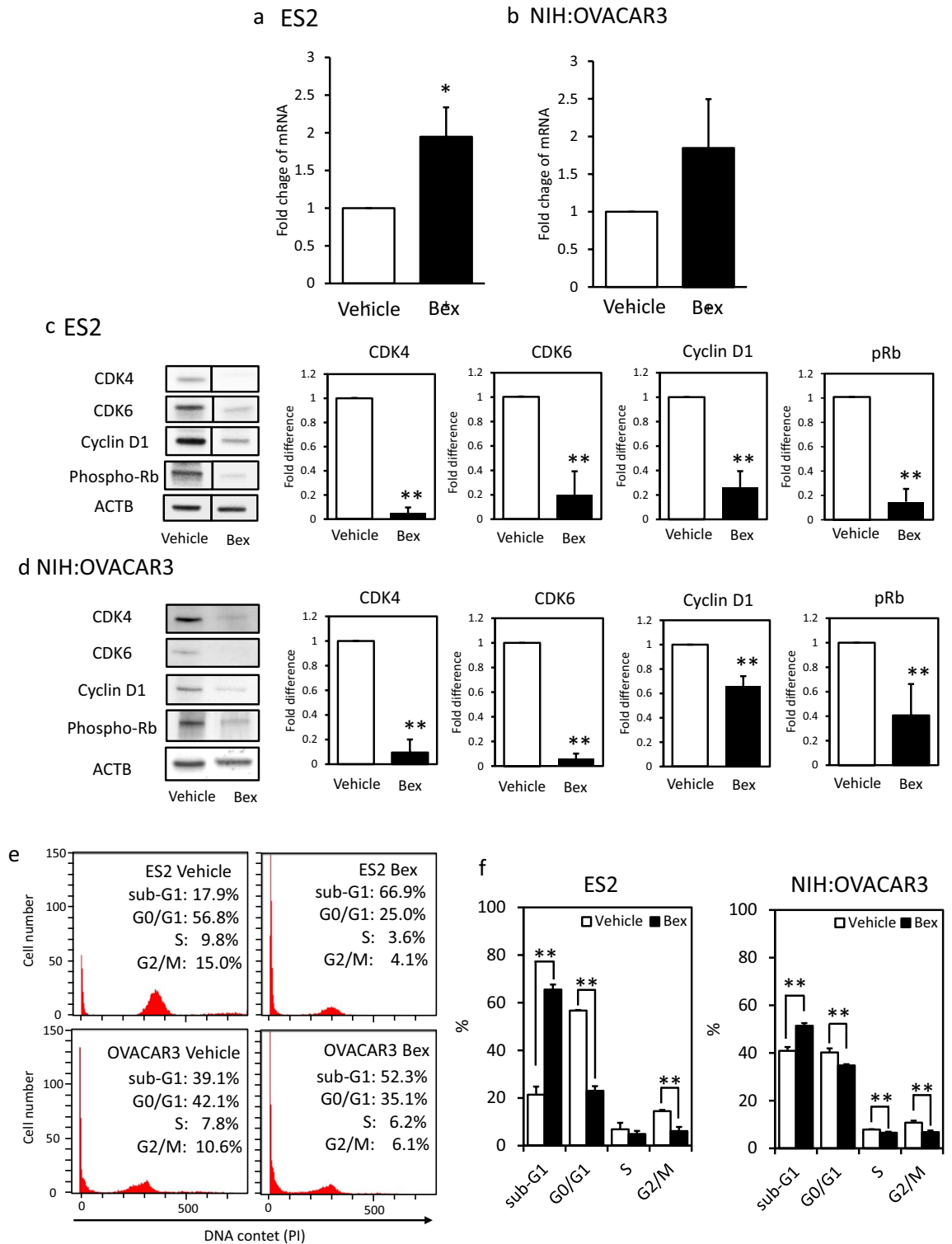


Figure 2. Bexarotene treatment increased CDKN1A mRNA expression, decreased cell cycle-related proteins, and increased the sub-G1 phase cell population. Levels of CDKN1A mRNA were measured and compared between 10 μ M bexarotene-treated cells and nontreated cells 24 h after bexarotene treatment in (a) ES2 and (b) NIH:OVACAR3 cells. CDKN1A expression was assessed using the $2^{-\Delta\Delta CT}$ quantitation method and normalized to housekeeping gene GAPDH using a no-treatment control as a calibrator. The results presented were mean, \pm standard deviation for at least three independent experiments. (c, d) Western blot analysis was performed to evaluate the effect of 10 μ M bexarotene on cell cycle-related proteins (CDK4, CDK6, cyclin D1, and phospho-Rb) in ES2 and NIH:OVACAR3 cells. Used as an internal control was β -actin. Columns and bar graphs represent the mean \pm standard deviation for at least three independent experiments. Quantification of protein levels was performed by densitometry and normalized to β -actin. (e, f) Cell cycle analysis with PI-stained cells. Bexarotene (10 μ M) treatment significantly increased the sub-G1 phase cell population and reduced G0/G1 and G2/M phase population in both the cell lines. White bars and the black bars represent the data in the vehicle- and 10 μ M-bexarotene treated cell, respectively. * $P < 0.05$, ** $P < 0.01$, compared with bexarotene-free control. ACTB, β -actin.

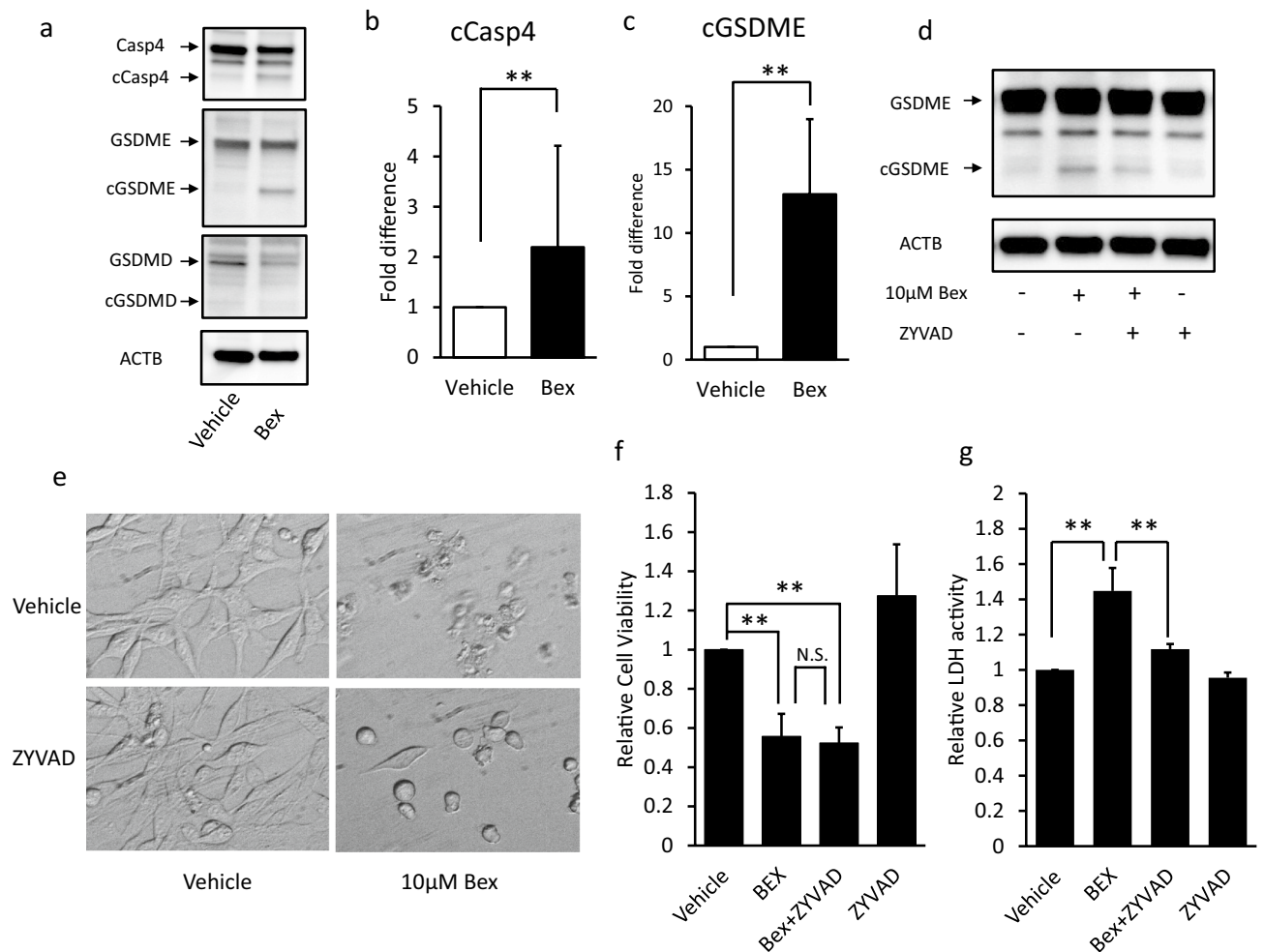


Figure 3. Bexarotene induces pyroptosis in ES2 cells. **(a)** Bexarotene increased pyroptosis-related proteins (Casp4, GSDME, and GSDMD) following exposure with 10 μM of bexarotene for 24 h in ES2 cells. Bexarotene increased cleaved caspase-4 levels **(b)** and cleaved GSDME levels **(c)**. B-actin was used as an internal control. **(d)** ZYVAD-FMK treatment reduced the levels of cleaved GSDME 4 h following bexarotene treatment. ES2 cells were pretreated with or without 10 μM-ZYVAD-FMK (caspase-4 inhibitor) 1 h before 10-μM-bexarotene treatment. **(e)** Bexarotene-treated cells showed pyroptotic-like morphological changes (upper right panel), whereas pretreatment with ZYVAD-FMK attenuated bexarotene-induced cell shape alteration (lower right panel). **(f)** Cell numbers were manually counted 24 h after bexarotene treatment, and cell viability against the bexarotene nontreated group was calculated. Pretreatment with ZYVAD-FMK could not suppress bexarotene-induced cell viability reduction. **(g)** The extracellular LDH levels increased by bexarotene were reduced by pretreatment with ZYVAD-FMK. Columns and bar graphs represent the mean ± standard deviation for at least three independent experiments. ** $P < 0.01$. Casp, Caspase; ACTB, β-actin; cGSDME, cleaved GSDME; cGSDMD, cleaved GSDMD; ZYVAD-FMK, ZYVAD; LDH, lactate dehydrogenase; N.S., not significant.

Discussion

This study revealed that bexarotene induced cell death in several ovarian cancer cell lines under a clinical setting concentration. Furthermore, this study clarified the following points: (1) bexarotene-induced cell death might be caused via pyroptosis mediated by caspase-4 activation and GSDME cleavage; (2) bexarotene suppresses cell proliferation through sub-G1 cell cycle arrest; and (3) bexarotene rapidly induced ER stress but might not be related to pyroptosis.

Our study confirmed that bexarotene (5–20 μM) induced cell death and inhibited cell proliferation in ovarian cancer cell lines. This experimental concentration of bexarotene almost has the same or lower concentrations than those of the clinical concentration (C_{max} : 10.4 μM, Targretin capsules 75 mg, interview form, Minophagen Pharmaceutical Co., Ltd., Zama, Japan). Conversely, the all-trans retinoic acid (ATRA) concentration, which is a well-investigated retinoic acid against ovarian cancer in vitro, has supraphysiologic concentrations. The ATRA concentration (sometimes as high as 10 μM) in in vitro studies was 5–50 times higher than that in the clinical setting (C_{max} : 0.18 μM, VESANOID Capsule 10 mg, interview form, Fuji Pharma Co., Tokyo, Japan). ATRA increases apoptosis and decreases cell proliferation, thereby proving effective against several ovarian cancer cell lines^{26–29}. In the study by Lokman et al.²⁹, the cell survival of two of five serous ovarian cancer cell lines (OVCAR-3 and OV-90) was inhibited by more than 20%; however, proliferation inhibition was weak or almost

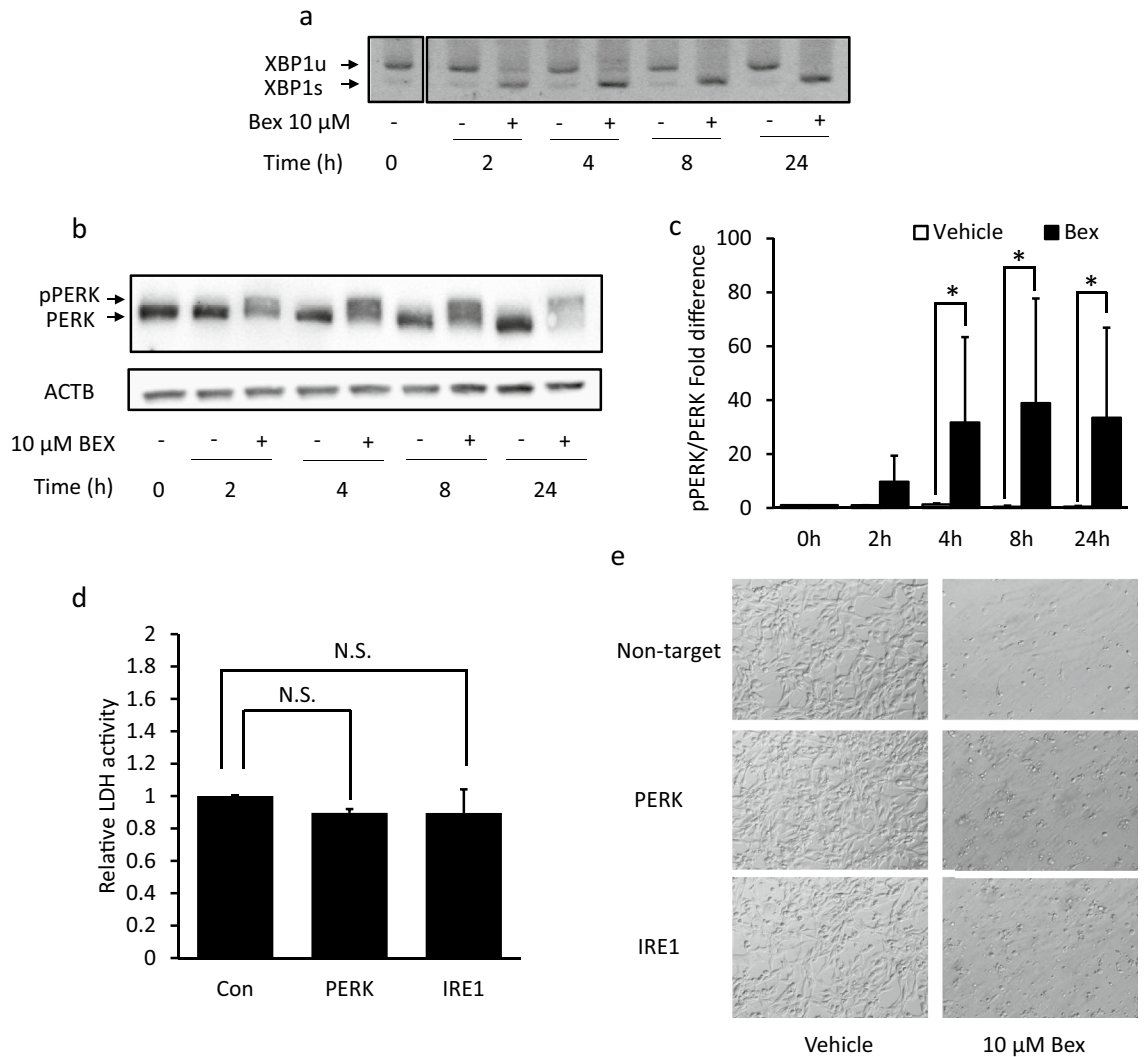


Figure 4. Bexarotene-induced ER stress, which is not associated with pyroptosis. Time-dependent changes in (a) XBP1 mRNA and (b, d) PERK protein levels following exposure to 10 μ M of bexarotene for 2–24 h. (a) The XBP1 mRNA splicing was upregulated in a time-dependent manner. (b, c) the molecular weight of PERK was rapidly altered to a higher molecular form (active form). (d, e) Control, PERK, or IRE1 siRNA-transfected cells were incubated for 24 h with 10 μ M of bexarotene. (d) After bexarotene treatment, extracellular LDH was measured and compared between the control group and each siRNA-transfer group. No significant differences in LDH activity were found between each siRNA-transfer group and the control group. (e) Morphological analysis of control, PERK, or IRE1 siRNA-transfer ES2 cell line. β -actin was used as an internal control. Columns and bar graphs represent the mean \pm standard deviation for at least three independent experiments. * $P < 0.05$, N.S., not significant.

nonexistent for the other three cells (OAW28, COV318, and COV362). In addition, several ovarian cell lines, such as COV362, COV318, SKOV-3, and CP70, are resistant to ATRA. Contrary to ATRA, bexarotene had the potential for clinical application in ovarian cancer.

We confirmed that bexarotene-induced cell death is pyroptosis mediated by caspase-4 activation and GSDME cleavage. RNA-seq analysis was performed using ES2 cells 24 h after the 10 μ M-bexarotene treatment (data not shown). No changes were observed in the caspases, except for caspase-4. Therefore, the other caspases were not involved in the mechanism of pyroptosis induced by bexarotene. As far as we know, this is the first report of bexarotene-induced death of pyroptotic cells in an ovarian cancer cell line. According to a research by Zhang et al., bexarotene induces apoptosis in CTCL cells³⁰. Apoptosis is characterized by many distinct morphological features, including cell shrinkage and fragmentation into membrane-bound apoptotic bodies³¹, and mediated by caspase-3 and -8 activation³². However, the characteristic morphology of apoptosis was not observed in bexarotene-treated ovarian cancer cell lines in ES2 cells and NIH:OVACAR3 cells. In addition, the extracellular activity of LDH, which is initially present intracellularly, is not elevated on apoptosis. This type of cell death featured cell proliferation, such as the morphological changes during pyroptosis³³. Pyroptosis is a proinflammatory programmed cell death typically induced by a viral infection, toxin, and chemotherapy drugs¹³. Three main pathways of inducing pyroptosis have been reported. The first is the canonical pathway of pyroptosis, which is

regulated by inflammation-activated caspase-1. The second is the non-canonical pyroptotic pathway regulated by caspase-4/5 in humans and caspase-11 in the mouse. GSDMD is a common substrate for caspase-1/4/5/11 for both canonical and non-canonical pyroptosis²³. The last pathway is mediated by caspase-3 and GSDME, which can be activated by chemotherapy drugs¹⁴. The study showed that bexarotene induced pyroptotic cell death through the caspase-4–GSDME-dependent signaling pathway in an ovarian cancer cell line. It is the first report demonstrating the induction of pyroptosis by caspase-4 activation and GSDME cleavage.

The anticancer effect of bexarotene was thought to be due to its genomic function as an RXR agonist. The ligand-activated RXR homodimer binds two RXR consensus domains within the promoter region of *CDKN1A* genes and upregulates the *CDKN1A* mRNA expression²⁰. In this study, bexarotene upregulated *CDKN1A*, which codes a cyclin-dependent kinase inhibitor p21, and downregulated cell cycle-related proteins downstream of p21. Therefore, bexarotene also acts as an RXR agonist in ovarian cancer cells. However, several studies indicated that the accumulation of p21 could induce growth inhibition and cell cycle arrest but could not induce cell death³⁴. Thus, the induction of *CDKN1A* alone could not explain bexarotene-induced cell death. However, in this study, bexarotene could induce cell death with characteristic morphological changes of pyroptosis through caspase-4 and GSDME. In addition, the knockdown of RXR α or RXR β by siRNA could not attenuate the LDH release induced by bexarotene (Supplementary Figure S1). These results suggested that the induction of pyroptosis through caspase-4 and GSDME was not mediated by RXR. Therefore, we speculated that bexarotene has genomic functions via RXR and non-genomic functions via caspase-4 and GSDME. These two actions were also considered independent. Furthermore, the cell-killing effect of bexarotene was observed at a clinical concentration (10 μ M); however, *CDKN1A* activation only showed a twofold change at this concentration. Therefore, bexarotene could have induced cell death by pyroptosis mediated by caspase-4 activation rather than by p21-mediated cell cycle arrest.

In this study, we also showed that the bexarotene-activated ER stress in ovarian cancer cells was consistent with the findings of a previous report wherein ER stress was induced in the human neuroblastoma cell line by a high concentration of bexarotene³⁵. Several studies have reported that ER stress can lead to pyroptosis^{24,25,36}. Palmitic acid and the ER stressor tunicamycin induce ER stress, leading to pyroptosis. An ER stress inhibitor can inhibit pyroptosis caused by palmitic acid or tunicamycin-induced ER stress. In this study, we have also demonstrated that the attenuation of ER stress by si-PERK and si-ERE1a could not restore bexarotene-induced pyroptosis, suggesting that bexarotene-induced pyroptosis is not mediated by ER stress in ovarian cancer cells. Hence, future research should investigate how bexarotene induces pyroptosis in ovarian cancer cells.

Conclusions

Our study showed that the clinical concentration of bexarotene reduces cell proliferation by inducing p21, which is still widely known and can also cause cell death, which is possibly pyroptosis, in ovarian cancer cell lines. Therefore, bexarotene is a potential anticancer drug for ovarian cancer. This study, however, was unable to elucidate the mechanisms of bexarotene-induced pyroptosis. Therefore, to better understand the pharmacological action of bexarotene, future research should further investigate the mechanisms of bexarotene-induced pyroptosis in ovarian cancer cells.

Data availability

All data analyzed in this study are included in this published article.

Received: 28 October 2021; Accepted: 22 June 2022

Published online: 01 July 2022

References

1. Siegel, R. L., Miller, K. D. & Jemal, A. Cancer statistics, 2019. *CA Cancer J. Clin.* **69**, 7–34. <https://doi.org/10.3322/caac.21551> (2019).
2. Boehm, M. F. *et al.* Synthesis and structure–activity relationships of novel retinoid X receptor-selective retinoids. *J. Med. Chem.* **37**, 2930–2941. <https://doi.org/10.1021/jm00044a014> (1994).
3. Gniadecki, R. *et al.* The optimal use of bexarotene in cutaneous T-cell lymphoma. *Br. J. Dermatol.* **157**, 433–440. <https://doi.org/10.1111/j.1365-2133.2007.07975.x> (2007).
4. Dragnev, K. H. *et al.* Bexarotene plus erlotinib suppress lung carcinogenesis independent of KRAS mutations in two clinical trials and transgenic models. *Cancer Prev. Res. (Phila)* **4**, 818–828. <https://doi.org/10.1158/1940-6207.CAPR-10-0376> (2011).
5. Esteva, F. J. *et al.* Multicenter phase II study of oral bexarotene for patients with metastatic breast cancer. *J. Clin. Oncol.* **21**, 999–1006. <https://doi.org/10.1200/JCO.2003.05.068> (2003).
6. Yen, W. C., Prudente, R. Y. & Lamph, W. W. Synergistic effect of a retinoid X receptor-selective ligand bexarotene (LGD1069, Targretin) and paclitaxel (Taxol) in mammary carcinoma. *Breast Cancer Res. Treat.* **88**, 141–148. <https://doi.org/10.1007/s10549-004-1426-5> (2004).
7. Yen, W. C. & Lamph, W. W. The selective retinoid X receptor agonist bexarotene (LGD1069, Targretin) prevents and overcomes multidrug resistance in advanced breast carcinoma. *Mol. Cancer Ther.* **4**, 824–834. <https://doi.org/10.1158/1535-7163.MCT-05-0018> (2005).
8. Yen, W. C. *et al.* A selective retinoid X receptor agonist bexarotene (Targretin) prevents and overcomes acquired paclitaxel (Taxol) resistance in human non-small cell lung cancer. *Clin. Cancer Res.* **10**, 8656–8664. <https://doi.org/10.1158/1078-0432.CCR-04-0979> (2004).
9. Tooker, P. *et al.* Bexarotene (LGD1069, Targretin), a selective retinoid X receptor agonist, prevents and reverses gemcitabine resistance in NSCLC cells by modulating gene amplification. *Cancer Res.* **67**, 4425–4433. <https://doi.org/10.1158/0008-5472.CAN-06-4495> (2007).
10. Yen, W. C. & Lamph, W. W. A selective retinoid X receptor agonist bexarotene (LGD1069, Targretin) prevents and overcomes multidrug resistance in advanced prostate cancer. *Prostate* **66**, 305–316. <https://doi.org/10.1002/pros.20347> (2006).
11. Song, J. I. *et al.* Abrogation of transforming growth factor- α /epidermal growth factor receptor autocrine signaling by an RXR-selective retinoid (LGD1069, Targretin) in head and neck cancer cell lines. *Cancer Res.* **61**(5919–5925), 11479234 (2001).

12. Shi, J. *et al.* Cleavage of GSDMD by inflammatory caspases determines pyroptotic cell death. *Nature* **526**, 660–665. <https://doi.org/10.1038/nature15514> (2015).
13. Yu, P. *et al.* Pyroptosis: Mechanisms and diseases. *Signal Transduct. Target. Ther.* **6**, 128. <https://doi.org/10.1038/s41392-021-00507-5> (2021).
14. Wang, Y. *et al.* Chemotherapy drugs induce pyroptosis through caspase-3 cleavage of a gasdermin. *Nature* **547**, 99–103. <https://doi.org/10.1038/nature22393> (2017).
15. Xia, X. *et al.* The role of pyroptosis in cancer: Pro-cancer or pro-“host”? *Cell Death Dis.* **10**, 650. <https://doi.org/10.1038/s41419-019-1883-8> (2019).
16. Tan, Y. *et al.* Pyroptosis: A new paradigm of cell death for fighting against cancer. *J. Exp. Clin. Cancer Res.* **40**, 153. <https://doi.org/10.1186/s13046-021-01959-x> (2021).
17. Kaiser, P. C., Körner, M., Kappeler, A. & Aebi, S. Retinoid receptors in ovarian cancer: Expression and prognosis. *Ann. Oncol.* **16**, 1477–1487. <https://doi.org/10.1093/annonc/mdi265> (2005).
18. Schmittgen, T. D. & Livak, K. J. Analyzing real-time PCR data by the comparative C(T) method. *Nat. Protoc.* **3**, 1101–1108. <https://doi.org/10.1038/nprot.2008.73> (2008).
19. Schneider, K. S. *et al.* The inflammasome drives GSDMD-independent secondary pyroptosis and IL-1 release in the absence of caspase-1 protease activity. *Cell Rep.* **21**, 3846–3859. <https://doi.org/10.1016/j.celrep.2017.12.018> (2017).
20. Tanaka, T., Suh, K. S., Lo, A. M. & De Luca, L. M. P21WAF1/CIP1 is a common transcriptional target of retinoid receptors: Pleiotropic regulatory mechanism through retinoic acid receptor (RAR)/retinoid X receptor (RXR) heterodimer and RXR/RXR homodimer. *J. Biol. Chem.* **282**, 29987–29997. <https://doi.org/10.1074/jbc.M701700200> (2007).
21. Kehn, K. *et al.* The role of cyclin D2 and p21/waf1 in human T-cell leukemia virus type 1 infected cells. *Retrovirology* **1**, 6. <https://doi.org/10.1186/1742-4690-1-6> (2004).
22. Zhang, Y., Chen, X., Gueydan, C. & Han, J. Plasma membrane changes during programmed cell deaths. *Cell Res.* **28**, 9–21. <https://doi.org/10.1038/cr.2017.133> (2018).
23. Feng, S., Fox, D. & Man, S. M. Mechanisms of gasdermin family members in inflammasome signaling and cell death. *J. Mol. Biol.* **430**, 3068–3080. <https://doi.org/10.1016/j.jmb.2018.07.002> (2018).
24. Lebeaupin, C. *et al.* ER stress induces NLRP3 inflammasome activation and hepatocyte death. *Cell Death Dis.* **6**, e1879. <https://doi.org/10.1038/cddis.2015.248> (2015).
25. Ke, R., Wang, Y., Hong, S. & Xiao, L. Endoplasmic reticulum stress related factor IRE1alpha regulates TXNIP/NLRP3-mediated pyroptosis in diabetic nephropathy. *Exp. Cell Res.* **396**, 112293. <https://doi.org/10.1016/j.yexcr.2020.112293> (2020).
26. Krupitza, G. *et al.* Retinoic acid induced death of ovarian carcinoma cells correlates with c-myc stimulation. *Int. J. Cancer* **61**, 649–657. <https://doi.org/10.1002/ijc.2910610511> (1995).
27. Wu, S. *et al.* All-trans-retinoic acid blocks cell cycle progression of human ovarian adenocarcinoma cells at late G1. *Exp. Cell Res.* **232**, 277–286. <https://doi.org/10.1006/excr.1997.3495> (1997).
28. Karabulut, B. *et al.* Enhancing cytotoxic and apoptotic effect in OVCAR-3 and MDAH-2774 cells with all-trans retinoic acid and zoledronic acid: A paradigm of synergistic molecular targeting treatment for ovarian cancer. *J. Exp. Clin. Cancer Res.* **29**, 102. <https://doi.org/10.1186/1756-9966-29-102> (2010).
29. Lokman, N. A. *et al.* Anti-tumour effects of all-trans retinoic acid on serous ovarian cancer. *J. Exp. Clin. Cancer Res.* **38**, 10. <https://doi.org/10.1186/s13046-018-1017-7> (2019).
30. Zhang, C. *et al.* Induction of apoptosis by bexarotene in cutaneous T-cell lymphoma cells: Relevance to mechanism of therapeutic action. *Clin. Cancer Res.* **8**(1234–1240), 12006543 (2002).
31. Saraste, A. & Pulkki, K. Morphologic and biochemical hallmarks of apoptosis. *Cardiovasc. Res.* **45**, 528–537. [https://doi.org/10.1016/s0008-6363\(99\)00384-3](https://doi.org/10.1016/s0008-6363(99)00384-3) (2000).
32. Shi, Y. Mechanisms of caspase activation and inhibition during apoptosis. *Mol. Cell* **9**, 459–470. [https://doi.org/10.1016/S1097-2765\(02\)00482-3](https://doi.org/10.1016/S1097-2765(02)00482-3) (2002).
33. de Vasconcelos, N. M. *et al.* Single-cell analysis of pyroptosis dynamics reveals conserved GSDMD-mediated subcellular events that precede plasma membrane rupture. *Cell Death Differ.* **26**, 146–161. <https://doi.org/10.1038/s41418-018-0106-7> (2019).
34. Almond, J. B. & Cohen, G. M. The proteasome: A novel target for cancer chemotherapy. *Leukemia* **16**, 433–443. <https://doi.org/10.1038/sj.leu.2402417> (2002).
35. Dheer, Y. *et al.* Bexarotene modulates retinoid-X-receptor expression and is protective Against neurotoxic endoplasmic reticulum stress response and apoptotic pathway activation. *Mol. Neurobiol.* **55**, 9043–9056. <https://doi.org/10.1007/s12035-018-1041-9> (2018).
36. Cheng, S. B. *et al.* Pyroptosis is a critical inflammatory pathway in the placenta from early onset preeclampsia and in human trophoblasts exposed to hypoxia and endoplasmic reticulum stressors. *Cell Death Dis.* **10**, 927. <https://doi.org/10.1038/s41419-019-2162-4> (2019).

Acknowledgements

We thank Enago (<http://www.enago.jp>) for editing and reviewing this manuscript for English language.

Author contributions

T.K., A.M., K.N., and M.S. conceived and designed the experiment while T.K., P.H., and M.S. performed the experiments. T.K., K.N., and A.M. wrote the article and conducted the analyses. All authors have read and approved the final manuscript.

Funding

The Japan Society for the Promotion of Science KAKENHI Grants 18K09282 helped fund this study.

Competing interests

The authors declare no competing interests.

Additional information

Supplementary Information The online version contains supplementary material available at <https://doi.org/10.1038/s41598-022-15348-7>.

Correspondence and requests for materials should be addressed to A.M.

Reprints and permissions information is available at www.nature.com/reprints.

Publisher's note Springer Nature remains neutral with regard to jurisdictional claims in published maps and institutional affiliations.



Open Access This article is licensed under a Creative Commons Attribution 4.0 International License, which permits use, sharing, adaptation, distribution and reproduction in any medium or format, as long as you give appropriate credit to the original author(s) and the source, provide a link to the Creative Commons licence, and indicate if changes were made. The images or other third party material in this article are included in the article's Creative Commons licence, unless indicated otherwise in a credit line to the material. If material is not included in the article's Creative Commons licence and your intended use is not permitted by statutory regulation or exceeds the permitted use, you will need to obtain permission directly from the copyright holder. To view a copy of this licence, visit <http://creativecommons.org/licenses/by/4.0/>.

© The Author(s) 2022